JOURNAL OF SPACECRAFT AND ROCKETS
Vol. 43, No. 4, July–August 2006

Investigation of Force-Limited Vibration for Reduction of Overtesting

Y. Soucy*
Canadian Space Agency, Saint-Hubert, Quebec J3Y 8Y9, Canada
and
V. Dharanipathi† and R. Sedaghati‡
Concordia University, Montreal, Quebec H3G 1M8, Canada

The force-limited vibration approach was developed in the 1990s to reduce overtesting associated with conventional vibration tests of aerospace hardware. Because of its numerous advantages, the semiempirical method is presently the most widely used method to derive the force limits. The configuration-dependent constant parameter C is one of the key parameters of the method. The main results and findings of a research and development project investigating the semiempirical method are presented. More specifically, the project investigated the range of values taken by C (or C^2) and the parameters on which it depends. The details and the results of an in-depth analytical sensitivity study with 134 different cases and the results of the experimental validation of the analytical procedures are included. The analytical sensitivity study shows that the C^2 value depends mainly on 1) the effective mass ratio between the test item and the mounting structure, at the fundamental frequency of the test item, 2) the number and position of the interface attachment points between the test item and the mounting structure, and 3) the direction of excitation. It also shows that the C^2 value is basically independent of the damping value for most configurations.

I. Introduction

FORCE-LIMITED vibration (FLV) testing is an improved test approach developed in the 1990s to reduce the overtesting associated with conventional vibration tests of aerospace hardware.[1,2] In addition to controlling the input acceleration as in conventional vibration testing, the FLV approach measures and limits the reaction force between the test item and the shaker. The FLV approach has been used successfully by the NASA Jet Propulsion Laboratory (JPL) during the past decade on numerous pieces of flight hardware at all hardware levels, including complete spacecraft. FLV testing is now applied routinely at JPL. Other NASA centers, for example, NASA Goddard Space Flight Center, NASA John H. Glenn Research Center at Lewis Field, and some U.S. companies have also implemented FLV testing on several flight missions. Recently, FLV testing has also been applied in Canada for four different missions. The approach has been validated with system-level acoustic tests (for subsystems and lower levels of assembly) and with some flight data.[3–6]

Estimation of the force limits is the most critical step of the FLV approach. The semiempirical method is presently the method most widely applied to derive the force limits between the test item and the shaker. The advantages of the semiempirical method over previously developed more analytical techniques, for example, the simple and complex two-degree-of-freedom system (TDFS) methods,[1,2] are significant and have greatly contributed to the widespread acceptance of the FLV approach presently taking place in the aerospace community.

Selection of the crucial configuration-dependent constant C, which sets the force limits throughout the frequency bandwidth of excitation, is based on the application of various criteria including, but not limited to, the extrapolation of interface forces for similar mounting structures and test items. Based on limited number of flight data,[3,4] it has been observed that in normal conditions C^2 value as low as 2 might be chosen for complete spacecraft or strut-mounted heavier equipment, and C^2 value as high as 5 might be considered for directly mounted lightweight test items.[7] Note that values outside that range have been reported in the literature. On the lower side, a C^2 value of 1 was selected for the Mars Exploration Rover spacecraft.[8] On the higher side, C^2 values of 8 and 10 were selected for the Fourier transform spectrometer (FTS) instrument of SCISAT-1 spacecraft.[9] As an extreme case, an equivalent C^2 value of 100 has been used for a very light 30-g (0.066-lb) assembly of the Hubble Wide Field Planetary Camera.[1]

The semiempirical method is very powerful and quite straightforward to apply for implementing force limiting. However, because of its partly empirical nature, there is still some work required to make everyone in the aerospace community comfortable with its application. The fact that only a few comparison results between force limits derived with the semiempirical method and interface force at higher hardware level of assembly exist in the literature led to the initiation of a research and development project for the investigation of the method. The project was a collaborative effort between the Canadian Space Agency (CSA) and Concordia University. The aim of the project was to provide some insight into the proper selection of C^2 values, especially for new users of the method. This paper presents the main results and findings of this investigation, focusing mainly on the range of values taken by C^2 and the parameters on which it depends.

The project included 1) performing design optimization with finite element analysis of test items, mounting structures, and fixtures; 2) conducting an in-depth analytical sensitivity study using 142 different cases; and 3) validating experimentally for selected cases the procedures used for the analytical study. In the present paper, 134 of these 142 cases are considered; 8 cases are removed for reasons explained in a later section.

Received 23 December 2004; revision received 9 November 2005; accepted for publication 28 November 2005.

*Senior Structural Dynamics Engineer, Space Technologies, 6767 route de l'Aéroport.

†M.S. Student, Department of Mechanical Engineering; currently Stress Analyst, CDI-Aerospace, 1000 Boul. St. Jean, Suite 715, Pointe Claire, QC H9R 5P1, Canada.

‡Assistant Professor, Department of Mechanical Engineering, 1455 de Maisonneuve Boulevard, West. Member AIAA.

II. Vibration Overtesting Problem

The main goal of random vibration testing of space hardware is to ensure that the structure will survive the launch environment. For practical reasons, the conventional practice for specifying the input excitation for vibration testing is to envelop the launch interface acceleration spectra. A certain amount of overtesting normally occurs because of the conservatism applied in enveloping of the environment itself. However, with this enveloping practice, the difference in boundary conditions between test and flight configurations becomes the main cause of vibration overtesting. During a vibration test, the test item is usually attached to a very rigid fixture and is excited or driven along a single linear direction, with the structure being completely restrained along the other five degrees of freedom (DOF). However, in the flight configuration, the test item is attached to a mounting structure, which normally exhibits some flexibilities in all six DOF in the frequency range of interest.

The flexibility difference in the direction of excitation is the main contributor to the overtesting phenomenon. In the flight configuration, the acceleration at the interface between the mounting structure and the test item drops at certain frequencies, resulting in valleys in the acceleration spectra. These frequencies correspond to the main resonance frequencies of the test item when attached to a rigid support (as on a shaker). This phenomenon is known as the vibration absorber effect. On the other hand, during a vibration test, the structure is excited with a specified input acceleration, which is the envelope of the flight interface acceleration, despite the amplitude drop in the flight configuration. This results in exaggerated amplification of input forces, and internal stresses, at the resonance frequencies of the test item, that is, overtesting.[1]

III. Estimation of Force Limits

A. Background

Impedance characteristics are related to input and response at single points on a structure. Strictly speaking, mechanical impedance refers to the ratio of input force divided by response velocity. However, in the literature, the name mechanical impedance is also given to the ratios force/displacement and force/acceleration.

One important impedance characteristic used in FLV testing is the apparent mass, defined as the mechanical impedance-type frequency response function (FRF) consisting of input force divided by acceleration. The force and acceleration of the apparent mass refer to the same DOF implying that it is a drive point FRF. The apparent mass can vary greatly with frequency and peaks at the resonance frequencies of the structure, as seen in Fig. 1 for the case of the single oscillator shown in Fig. 2. The oscillator has a mass m of unity and a dynamic amplification factor Q of 20. The abscissa of Fig. 1 is the frequency, normalized by the oscillator resonance frequency f_0.

For both the flight configuration with the test item coupled with the flexible mounting structure and the vibration test configuration

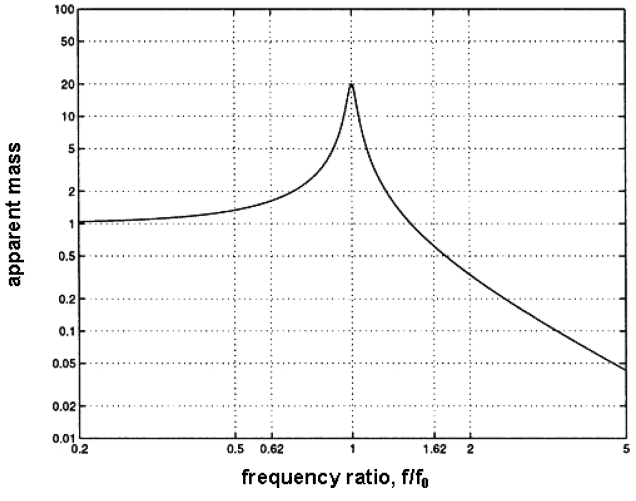

Fig. 1 Apparent mass of a single oscillator.

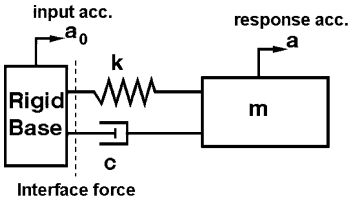

Fig. 2 Single oscillator in vibration test configuration.

with an isolated test item, the interface force spectral density [or power spectral density (PSD)] S_{ff} is related to the interface acceleration spectral density S_{aa} and the apparent mass M of the test item as follows[1]:

$$S_{ff}(f) = |M(f)|^2 S_{aa}(f) \tag{1}$$

Equation (1) is really the second law of Newton applied to the random vibration. The f is used to emphasize the frequency dependence of both the spectral densities and the apparent mass. Unfortunately, the precise analytical approaches to obtain the parameters defined in Eq. (1) are not practical, due to structural complexities of space vehicles.[7] The primary difficulty in using Eq. (1) to derive force limits is that the equation has to be evaluated at the coupled system resonance frequencies, which are generally unknown. Consequently, the difficulty in deriving the force limits from Eq. (1) has led to the development of more practical techniques, including the semiempirical method, which is the most widely used approach for the reasons provided in the Introduction.

B. Semiempirical Method

The basic idea behind the semiempirical method is to envelop properly the input force spectrum at the fundamental frequency of the test item. The random vibration form of the semiempirical method is given by the following two relations[2]:

$$S_{ff}(f) = C^2 M_0^2 S_{aa}(f), \qquad f < f_0 \tag{2}$$

$$S_{ff}(f) = C^2 M_0^2 S_{aa}(f)/(f/f_0)^n, \qquad f \geq f_0 \tag{3}$$

where S_{ff} is the sought limit to the force spectral density, S_{aa} is the defined input acceleration spectral density, M_0 is the physical mass of the test item, f_0 is the fundamental frequency (or frequency of the first significant mode), C is a configuration-dependent constant, and n is a roll-off ratio.

The C parameter is included in the equations to account for the vibration absorber effect taking place at the primary mode frequencies of the test item when attached to a flexible mounting structure, as discussed earlier. A physical interpretation of C may be obtained by comparing Eq. (2) with the figure of normalized force limits derived from the simple TDFS model of the coupled system, in which an oscillator representing a mode of vibration of the test item is coupled with another oscillator representing a mode of vibration of the mounting structure.[2] It is then shown that the dynamic amplification factor Q of the isolated test item is replaced by C. A lower C value results in lower force limits, implying a more significant vibration absorber effect.

In Eqs. (2) and (3), the mass M_0 is known, S_{aa} is defined, the value of f_0 may be obtained from finite element (FE) analysis and finalized from a low-level sine or random run performed just before the full-level vibration testing.

As shown in Eq. (1), the force spectral density is proportional to the amplitude squared of the apparent mass of the test item. Also, as observed in Fig. 1 for a single oscillator, the apparent mass is falling off beyond the fundamental frequency. The rolloff ratio n in Eq. (3) is introduced to account for the falling off of the apparent mass. The value of n may also be obtained from FE analysis and finalized from the low-level sine or random run performed just before the full-level vibration testing. It is normally estimated between 1 and 3.

The constant C (or C^2) is a key parameter of the semiempirical method, which sets the force limits throughout the complete frequency bandwidth of excitation. The Introduction of the present paper contains a discussion on the range of values it might take

in ordinary circumstances. However, C is the only parameter of Eqs. (2) and (3) that cannot be obtained directly or from a low-level sine or random run. Some engineering judgment must be exercised to choose the value of C^2. In fact, the level of conservatism of the force limits depends on the selected value for C^2.

In real-life applications, selection of the value of C^2 may be based on any, or a combination, of the following criteria:

1) Interface force data may be extrapolated from similar mounting structures and test items.

2) A comparison may be made with force limits at the fundamental frequency derived from the more analytical simple and/or complex TDFS methods, when such predictions are available.[2,9] Normally, this comparison is not possible when the test item is the complete spacecraft because the requested impedance information for the mounting structure, that is, the launch vehicle, is not readily available.

3) A comparison may be made with quasi-static limit load. The selection of C^2 should ensure that the center of gravity acceleration (derived from the force PSD) does not exceed the limit load.[2,7]

4) A value for C^2 may be selected that results in a level of notching at the fundamental frequency equivalent to the notching provided by the mechanical impedance correction technique.[10] In fact, this criterion may lead to quite conservative force limits.[11]

5) The amount of clipping of the force PSD peak at the fundamental frequency may be assessed from low-level run. This criterion may be used as a guideline for a range of acceptable C^2 values, considering that the application of force limiting should not result in excessive clipping of the force PSD.[12] Although the use of this guideline requires a certain amount of engineering judgment, it can be quite useful, especially when the other criteria are not readily applicable.

6) A comparison may be made with interface force between the test item and the mounting structure for the launch configuration, when such information is available. The force limits should obviously be higher than the interface force to avoid any undertesting.

Another important point may be made from the observation of Eqs. (2) and (3) in the sense that the force limits derived from the semiempirical method (as well as from the TDFS methods) are proportional to the input acceleration specification. Consequently, any conservatism in enveloping the interface acceleration spectra is carried over to the force specification. The aim of FLV is only to account for the input notching due to the vibration absorber effect, not to compensate for overconservatism in defining the input acceleration envelope.

IV. Overview of the Project

As seen in the preceding section, the only parameter that may not be obtained directly or from a low-level preliminary run is the C^2 parameter. On the other hand, this constant is the critical parameter because the level of conservatism of the force limits depends on the selected value for C^2.

The main objective of the reported project was to investigate the range of C^2 values that might be normally expected and the parameters on which they depend. This objective was achieved through an in-depth analytical sensitivity study of C^2 using structures (test item and mounting structure) having a broad range of structural and dynamic properties and different interfaces.

The project consisted of several tasks as now summarized. The design requirements for the structures (test item and mounting structure) were defined in the first task. The key requirements are presented in the next section. Once the requirements were finalized, a great deal of effort was expended for the second task related to the design and FE analysis of the test items and mounting structures meeting these requirements. This part of the work involved performing a sensitivity study of the changes in dynamic properties of the individual structures with respect to changes in their structural properties and in the interface attachment points between them. This task also included the design of the fixtures for the experimental part of the work. As reported in Ref. 13, a larger amount of effort than expected was required to develop the proper fixture for testing in the vertical direction. The third task was the analytical sensitivity study related to C^2 and an investigation of the parameters on which it depends. It also naturally led to a study of the amount of input acceleration notching resulting from force limiting. Manufacturing of the hardware (test item, mounting structure, and fixtures) was another task of the project done essentially in parallel with the third task. The last task of the work consisted in performing some experimental work for selected cases of the analytical study (sometimes with minor modification of the structures for practical considerations) to validate the procedures applied in the analytical study.

V. Design for the Structures

A. Design Requirements

To meet the project objectives, design requirements for the structures (test item and mounting structure) were defined. Some of these requirements were required to respect the limitations of the vibration test facilities of CSA Space Technologies in St-Hubert, Quebec, Canada, for the experimental validation of the procedures for the analytical study. A total of 24 requirements were defined.[13] The key requirements included the following:

1) The test item and the mounting structure shall have provision for different combinations of attachment points between them. The maximum number of attachment points shall be 12.

2) The fundamental frequencies of the test item should be higher than 100 Hz, and the frequency of its first three major modes in each direction shall be no more than 600 Hz.

3) To simulate real-life situations, at least the first three resonance frequencies of the mounting structure shall be below the fundamental frequencies of the test item.

4) To simulate real-life situations, some of the design configurations shall contain several closely spaced modes for both the test item and the mounting structure, and these modes shall be coupled together.

5) It should be possible to modify the structural flexibility of both structures, to simulate a wide range of values for the most significant effective masses and their associated resonance frequencies.

6) The design of both the test item and the mounting structure shall allow the attachment of various numbers of rigid (lumped) masses at different locations. These lumped masses are to represent high-frequency components attached to the structures.

B. Design of the Test Item

Several iterations were required to come up with a design of the test item that would meet all design requirements. Details of the dynamic characteristics of the structure and of various design iterations are presented in Ref. 13.

The test item was designed as a hollow cube of $11 \times 11 \times 11$ in.^{3} with a wall thickness of 0.25 in. on each side. Two sides of the cube were removed to have easy access to the interior of the structure, for the experimental part, to add lumped masses (Fig. 3). The dimensions of the test item were selected on the basis of various requirements, including the dimensions of the shaker and the slip table. The wall thickness was derived from static and dynamic analysis to meet the requirements related to the mass and the fundamental

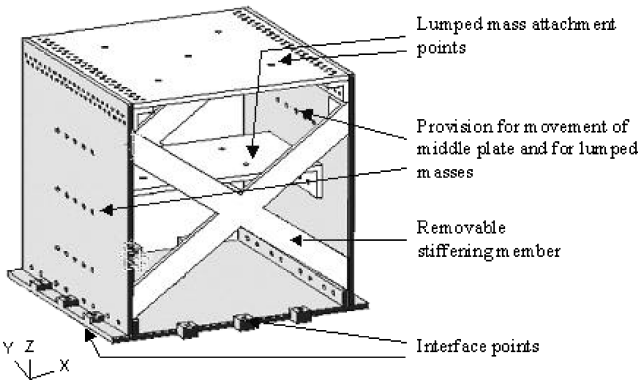

Fig. 3 Test item with provision for lumped mass attachment.

frequencies of the test item. All of the walls have the same uniform thickness to reduce the manufacturing cost and time.

To meet the requirements to simulate the dynamics and dynamic interaction of real space hardware, a plate was added in the middle of the cube connecting the two sidewalls. Its thickness and width are 0.25 and 5.5 in., respectively. This plate also supported the attachment of lumped masses. As shown in Fig. 3, hole patterns on the sidewalls allowed moving up and down the middle plate, as an increase in design flexibility. Through its own dynamics, its structural interaction with the cube, and its provision for attachment of lumped masses, the insertion of the middle plate significantly increased the design flexibility and, thus, the range of dynamic characteristics of the test item. This directly led to a larger number of possible cases for the sensitivity study of the C^2 coefficient.

For excitation in the X axis along which the structure is most flexible, additional stiffness to the test item was required to meet the fundamental frequency requirement. This was achieved through the addition of a 0.25-in.-thick and 1-in.-wide bar as a stiffening member connecting the top right corner to the bottom left corner, on each side on the cube. For some cases involving the addition of lumped masses, the simple bars were not sufficient, and they were replaced by $\times$-shape plates connected on each of the two sides of the structure, as shown in Fig. 3. The arms of the $\times$ have the same cross-sectional dimensions as the simple bars. For the cases for which the attachment points are moved from the vertical wall sides to the stiffening member sides and with all of the lumped masses, higher stiffness was provided by replacing the stiffening members by four 3/16-in.-thick brackets (one at each corner) connecting the base and the walls of the test item. Also, two stiffeners were added underneath the middle plate.

All plates making up the cube of the test item, the middle plate, and the various types of stiffening members were made with 6061 grade aluminum. The lumped masses were manufactured with brass material due to its higher density and, thus, smaller volume for the same weight.

Depending on the cases (without or with lumped masses), the weight of the test item varied from 15.7 to 45.4 lb and its fundamental frequency varied from 97 to 324 Hz. These numbers, thus, confirm that the retained design for the test item is quite versatile and definitively suitable for the subsequent analytical sensitivity study.

The FE software Patran[14]/Nastran[15] was employed to create the model and perform the analysis to obtain the final dimensions of the structures based on the design requirements. To perform random analysis, advanced tools of Nastran and the Structural Analysis Toolkit of Maya Heat Transfer[16] were used. The same tools were used to perform the analytical sensitivity study. Static analysis with quasi-static loads and random analysis of the coupled system were performed to verify the stresses at the design level, that is, 10-g rms specification from the general environmental verification specification (GEVS) discussed later. Stresses, forces, and accelerations at the critical locations were, thus, computed. The results obtained were used to perform the fatigue analysis to verify if the structure would withstand the numerous tests to be performed on it.

C. Design of the Mounting Structure

Different concepts were considered and several iterations were performed to develop the design of a mounting structure that would meet all of the requirements in terms of its physical properties (maximum mass and dimensions) and dynamic characteristics while exhibiting acceptable stresses for the specified 10-g rms base random excitation. The final concept consists of the mounting structure being designed as a structure similar to the test item. However, it is much more flexible than the test item to be representative of typical real-life situations.

When the dimensions of the slip table and the test item are taken into account the mounting structure is made up of a plate of 16×18 in. mounted on walls of 5-in.-high and 18-in.-long plates. The thickness of the plates was selected after performing the dynamic and static analysis of the structure to satisfy the requirements in terms of fundamental frequency. To further respect the requirement of having at least three resonance frequencies below the fundamental frequencies of the test item and to increase its dynamic interaction with the test item, a plate of dimensions 16×16 in. was attached across the length at midheight as shown in Fig. 4. The 12 holes in the top plate allowing the attachment of the test item with M6 bolts are clearly visible in Fig. 4. The top and middle plates, as well as the side plates, all have provision for the attachment of lumped masses.

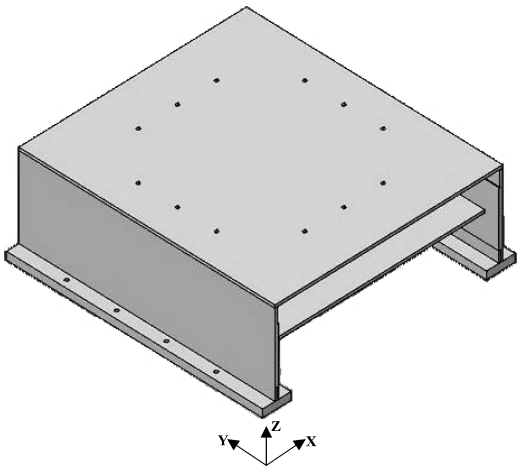

Fig. 4 Mounting structure.

The top plate was designed with variable thickness to increase further the structural flexibility of the mounting structure in the vertical direction (normal to the plane of plate) and to provide even more dynamic interaction with the test item. The thickness of the top plate varies from 1/8 in. at the center (covering the outer part of a cross section 10×10 in.) to 3/8 in. at the attachment points of the test item to the mounting structure. The thickness of the sidewalls connecting the top plate to the legs also varies across its height, to reduce the resonance frequencies of the mounting structure in the lateral and vertical directions. The thickness of the sidewall plate at the point of attachment to the top plate is 3/16 in. up to a depth of 1 in., whereas the rest of the sidewall plate has a thickness of 0.25 in.

The thickness of the middle plate is 3/16 in. to allow the maximum lumped mass at the highest test level (10-g rms). However, with this thickness for the middle plate, the frequency of the mounting structure involving this plate was found to be above the fundamental frequency of the test item, thus, violating the requirement of having multiple modes below the fundamental frequency of the test item. To reduce the stiffness of the middle plate, its attachment area with the sidewalls was reduced by removing a 4×8 in. surface of material on each side. This was done taking into account the stresses at the attachment points, which increased due to reduced contact area.

Almost the entire mounting structure (except the middle plate) was manufactured using 7075 grade aluminum, whereas regular 6061 grade was used for manufacturing the middle plate. Because of the higher yield strength of the 7075 material compared to the 6061 grade, the margin of safety of the structure was improved without increasing the mass of the structure because the density of both materials is the same.

Although the described design for the mounting structure with all dimensions mentioned had the required resonance frequencies below the fundamental frequencies of the test item and met almost all of the dynamic and static/physical requirements, the weight of the mounting structure was for certain cases below the weight of the test item. To increase the weight of the mounting structure, a brass plate of 6.6 lb (3 kg) and $6 \times 6 \times 0.7$ in.^{3} in dimensions was attached at the center of the top plate (facing the middle plate to have a flat top surface for easy attachment of the test item). This also helped in further reduction of fundamental frequencies and generation of multiple modes below the fundamental frequencies of the test item.

The mounting structure weighs 21.9 lb without any lumped mass and up to 61.5 lb when fully loaded with brass lumped masses. The fundamental frequency of the mounting structure varies between

35 and 83 Hz depending on the presence and distribution of lumped masses, as well as on the number of attachment points on the legs fixing the mounting structure to a rigid base (maximum of 16).

VI. Analytical Sensitivity Study

In this section, first the parameters are defined with respect to which the C^2 values were studied. The section then proceeds with a numerical example to present a detailed description of the procedures applied in each case for estimating the corresponding C^2 value. This is followed by a presentation of the key findings of the study. Finally, the section includes some discussion on the observed notching of the input acceleration PSD. All details of the study are reported in Ref. 13.

A. Sensitivity Parameters

Some guidelines were defined to select the cases for the analytical study to avoid duplication of the key parameters of the individual structures (test item and mounting structure) and of the assembled structures. In the present paper, a total of 134 different cases are considered. The parameters varied during the study were damping values, direction of excitation (three orthogonal directions), number and position of the interface attachment points (3, 4 , 6, 8, and 12 considered), stiffness of the structures, and pertinent effective and residual mass ratios of the structures.

The analysis was repeated for two different values of Q, namely, 20 and 50. Consequently, a total of 67 different configurations are considered with respect to the other parameters. It is realized that a Q of 50 might not be representative of the amplification factor expected at the spacecraft level. However, such a high value may be encountered at component and subsystem levels.

Test items having significantly different stiffness characteristics were combined with the mounting structures. The stiffness of the test item was controlled through the insertion of one or more stiffening components discussed earlier and some others described in Ref. 13. The study also investigated the effect of adding lump masses, in different amount and positions, for both the test item and the mounting structure. The stiffness and lumped mass variations resulted in changes in the resonance frequencies of both structures and, consequently, in different dynamic interaction between them.

B. Description of Procedures

The procedures for estimating the C^2 values are now described. A high-level description is first presented followed by an example to clarify some of the details of the procedures. These procedures were used throughout the analytical sensitivity study. For each case considered, the purpose of the procedures is to compute the so-called exact C^2 value that leads to a force limit corresponding to the relevant maximum interface force at the coupled system level.

The procedures consist of the following steps:

1) Obtain the apparent mass and the fundamental frequency (or frequency of the first significant mode) of the test item by applying a random white noise acceleration to the base of the test item sitting on a rigid base (fixture), over a frequency range of 20–2000 Hz.

2) Perform a coupled load analysis of the system. The same environment is imposed at the base of the mounting structure for all cases. The interface force and acceleration PSDs are then derived for each of the attachment points between the test item and the mounting structure.

3) Compute the total interface force PSD from the individual interface force PSDs.

4) With use of the maximum system level force and acceleration, compute the exact C^2 value.

5) Compute the notching of the input profile resulting from force limiting.

For the example selected for providing details of the procedures, the test item is fixed at four attachment points located on the sides of the sidewalls. The structure has cross plates as the stiffening members and no stiffeners underneath the middle plate. Thus, it corresponds to the design shown in Fig. 3. The test item has a total weight of 34.6 lb, including 18.9 lb of lumped mass distributed on top and middle plates. The mounting structure has a total weight of 61.5 lb, including 39.6 lb of lumped mass. The axis of excitation is the vertical Z direction.

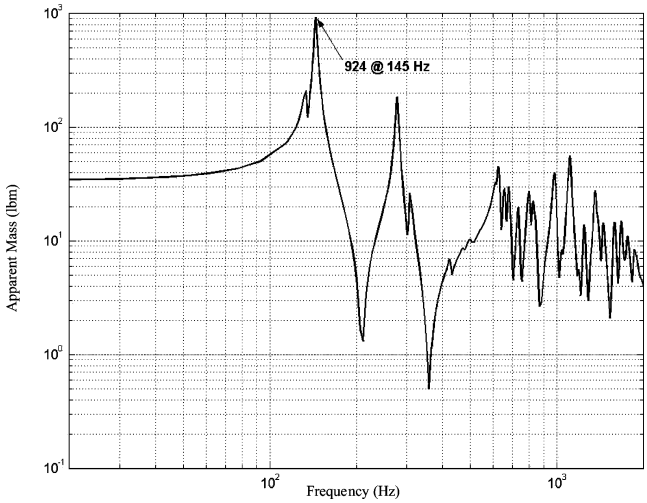

Fig. 5 Apparent mass of test item.

The apparent mass of the test item is shown in Fig. 5. The frequency of the fundamental mode in the direction of excitation is seen to be 145 Hz. The corresponding global mode shape is driven by the top and middle plates moving in phase up and down. The mode at 141 Hz represented by the smaller peak on the left-hand side of the main peak is found to correspond to a global mode mainly along the cross-axis Y direction.

For some cases of the analytical study, the apparent mass had a different profile than a textbook example with the peak being the largest at the fundamental lowest frequency and the subsequent peaks having decreasing height with the increased order of the modes. In fact, for a few cases, the apparent mass had two or more large peaks for the first modes, with the first mode not always being the highest peak. For these cases, the fundamental mode with frequency f_0 was chosen as the peak that seemed to be more appropriate to be conservative and not eliminate too much of the subsequent high level peaks when applying Eq. (3). This process of fundamental mode selection, which sometimes requires some engineering judgment, was performed as if we were dealing with real-life situation with all its implications, that is, the first peak was not systematically selected as the fundamental mode in the context of the semiempirical method.

For the coupled load analysis of step 2, the test item is fixed to the mounting structure at the same attachment points that are used in the evaluation of apparent mass. When the FE solver and its random vibration module are used, an environment is imposed at the base of the mounting structure. The acceleration input profile applied to the system is taken from NASA GEVS standard for the acceptance level vibration test performed on structures having 50 lb (22.7 kg) or less.[17] This profile has a rms value of 10.0 g in the range 20–2000 Hz. It is defined as a constant value of 0.08 g^2/Hz in the range 50–800 Hz, with a ± 6 dB/octave slope on each side of that range. For simplicity and because the derived C^2 value is independent of the coupled system input acceleration for the assumed linear structures, this profile was used for all cases, although some of the systems, such as the one of the present example, weighted more than 50 lb.

The value of the exact C^2 parameter is obtained from Eq. (2), which is rewritten here as

$$C^2 = \frac{S_{FF}(f_{\max f})}{S_{AA}(f_{\max a}) \times M_0^2} \tag{4}$$

where $S_{AA}(f_{\max a})$ is the maximum value of all the interface point accelerations at frequency $f_{\max a}$ occurring at the highest of the two relevant peaks adjacent to the antiresonance related to the fundamental frequency of the test item by itself. The relevance of such two adjacent peaks is discussed in Ref. 1 in relation with the vibration

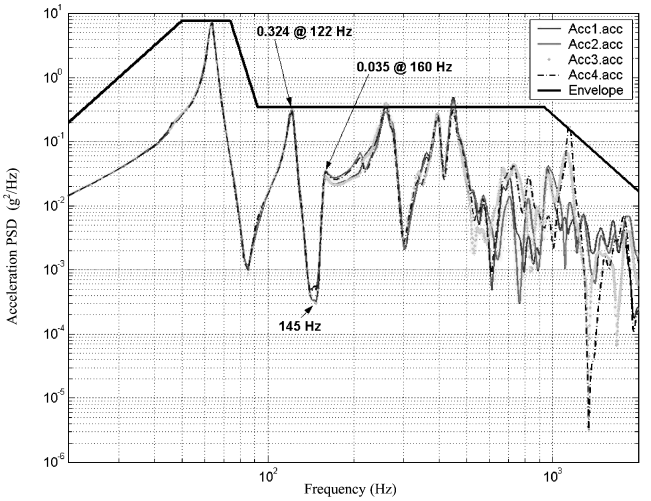

Fig. 6 Interface acceleration at four attachment points and envelope of accelerations.

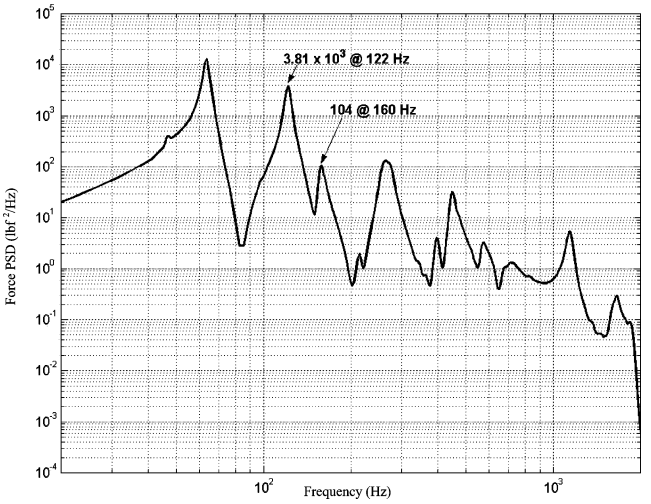

Fig. 7 Total interface force PSD at system level.

or dynamic absorber effect. In Eq. (4), $S_{FF}(f_{\max f})$ corresponds to the value of the total interface force PSD calculated at the frequency $f_{\max f}$ occurring at the higher of the two peaks adjacent to the antiresonance. The definition of the interface force PSD computed in step 3 of the procedures will be discussed later. For the majority of cases considered in the analytical study, the frequencies $f_{\max a}$ and $f_{\max f}$ are the same, implying that the maximum acceleration and force are occurring at the same mode at the system level.

For the present example, the dynamic amplification factor Q is set at 20, that is, damping ratio of 0.025. The interface acceleration between the test item and the mounting structure is computed at each of the four attachment points, and the PSDs are shown in Fig. 6. In this example, the antiresonance occurs at 145 Hz, and the maximum acceleration having a value of 0.324 g^2/Hz occurs at 122 Hz. This procedure for selecting the acceleration value implies that, in the frequency range of interest, the enveloping process for defining the input environment for testing the test item perfectly envelopes the highest peak of the interface accelerations directly relevant to the fundamental mode of the test item by itself. For frequencies away from the fundamental frequency of the test item, the acceleration envelope is defined by simply loose enveloping of the maximum interface accelerations. The acceleration envelope that would be used as the input environment for the test item is also shown in Fig. 6.

Step 3 of the procedures consists of computing the total interface force PSD at the coupled system level. This force PSD for the present example is shown in Fig. 7. For each frequency of the PSD, the interface force is obtained by adding the force at each of the interface points. Because the interface force at each of the attachment points is in the form of a PSD, that is, power, they cannot be added directly to represent the total force (TF) PSD. Hence, the TF PSD is defined as the square of the sum of square root of each individual force PSD, that is,

$$\text{TF(PSD)} = \left[\sum_{i=1}^{n} \sqrt{F_i\,(\text{PSD})}\right]^2 \tag{5}$$

where TF is the total force PSD at the interface level, n is the number of attachment points, and F_i is the individual force PSD at each attachment point.

In fact, Fig. 7 does not represent the true interface force in terms of amplitude at all frequencies of the PSD. The reason is that the forces are added by making the assumption that they are always in-phase, which is certainly not true at all frequencies. However, for the cases considered, they were found most of the time to be in phase for the mode at the resonance frequency $f_{\max f}$ used for computing the value of C^2. It has been verified for the current example that all interface forces are in phase at $f_{\max f}$. This verification is done by checking the mode shape of the coupled structure and the phase of the interface forces at $f_{\max f}$. For the few cases when some of the interface forces were not in phase with the remaining ones, this was taken into account by subtracting the corresponding terms in Eq. (5), instead of adding them as in the equation. This procedure for deriving the total interface force PSD at $f_{\max f}$ is in line with the process through which the same PSD would be obtained during a FLV test: Individual forces from the force sensors are first added (or subtracted) to obtain the total time-domain signal, then the PSD of the total force is computed by the vibration system. In a test, the phases add themselves properly in real time.

The described procedure for deriving the total interface force PSD at $f_{\max f}$, including subtraction of terms for the out-of-phase individual forces, is applicable in the cases when there is no closely spaced modes to the one at $f_{\max f}$, that is, the adjacent modes are far away enough so that their related force PSD contribution at $f_{\max f}$ are not significant compared to the total force PSD contribution of the mode at that frequency. Further investigation of the total interface force PSDs after publication of Refs. 11, 13, and 18 revealed that the adjacent peaks have negligible effects at $f_{\max f}$ for 134 of the 142 cases investigated. Consequently, for the present paper, only the 134 cases for which Eq. (5) is fully applicable are retained. This is a reduction in the number of cases compared with the original study of less than 6%.

The C^2 value, estimated in step 4 of the procedures, is obtained from Eq. (4). For the current example, this gives

$$C^2 = \frac{3.81 \times 10^3}{(0.324 \times 34.6^2)} = 10 \tag{6}$$

The values of maximum acceleration and force as defined earlier lead to an exact value for the estimation of C^2 parameter. This value is exact in the sense that the application of Eq. (2) using this value of C^2 together with the acceleration envelope covering exactly the interface acceleration PSDs at $f_{\max a}$ will result in a force-limit value equal to the maximum interface force at the system level relevant to the vibration absorber phenomenon. This implies that no overtesting or undertesting is involved in the process. Consequently, the selection of any C^2 larger than this exact value would lead to overtesting of the test item. Furthermore, if the acceleration enveloping process leads to an input acceleration higher than the maximum peak value discussed earlier, overtesting would be present even if the exact C^2 value was used.

Having obtained the value for C^2, the test item may now be tested by itself. The envelope of the interface accelerations at the coupled system level forms the input environment for the test item. During the actual FLV test (or its analytical simulation), the acceleration input is notched at, and around, the fundamental frequency and the frequency of the other significant modes where the total force at the base of the test item exceeds the force limits for the corresponding

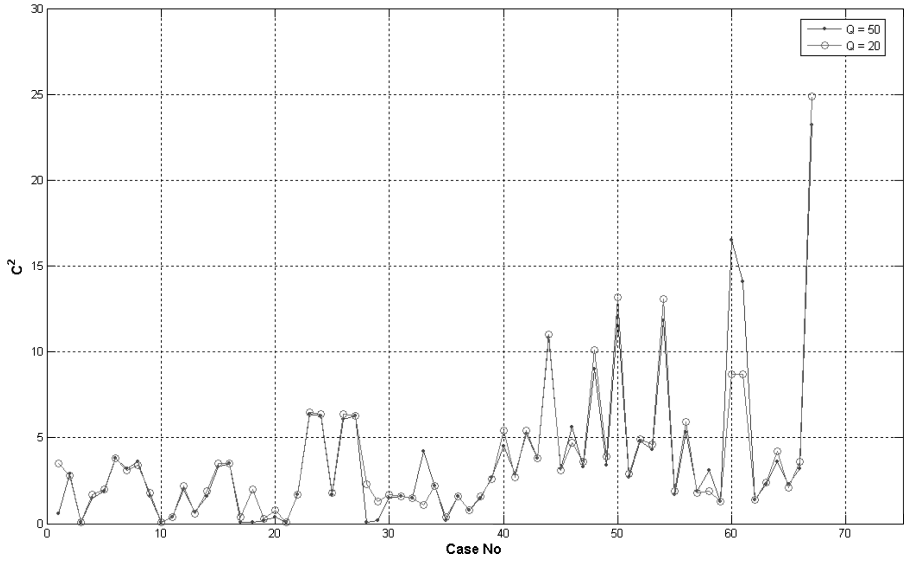

Fig. 8 C^2 values for two different Q values.

frequencies. The value of the acceleration notching at the fundamental frequency can be obtained by dividing the force limit with the unnotched force value of a test without FLV. From Eq. (1), the unnotched force is given by the product of the acceleration specification (maximum interface acceleration) and the square of the apparent mass at the fundamental frequency. For the current example, the notching value is

$$N = 10 \times \log\left[\frac{S_{FF}(\text{with FLV})}{S_{FF}(\text{without FLV})}\right] = 10 \times \log\left[\frac{3.81 \times 10^3}{[0.324 \times 924^2]}\right]$$

$$= -18.6\,\text{dB} \tag{7}$$

In this example, the apparent mass of the test item at the fundamental frequency is 924 lb, as shown in Fig. 5, the input acceleration is 0.324 g^2/Hz, and the force limit is 3.81×10^3 lbf^2/Hz.

C. Analysis Results and Discussion

This subsection presents the key results and findings of the analytical sensitivity study. More details of these results are reported in Ref. 13. However, note that following the publication of Ref. 13 and its related high-level summary presentation,[18] some additional data processing and analysis were performed that led to slight modification of some of the published results in these two references. The additional effort was performed as part of complementary work for comparing, for some cases, the system-level interface force with the force limits derived from the more analytical simple and complex TDFS methods.[19]

As mentioned before, a total of 134 different cases are considered in this paper. These cases consist of 67 different configurations studied for two different values of damping (Q of 20 and 50). These configurations are distributed among the directions of excitation as follows: 24 along the X axis, 5 along the Y axis, and 38 along the vertical Z axis.

First, let us consider the value of C^2 as a function of damping of the test item. Figure 8 presents a graph of the C^2 values for each of the two Q values, as a function of the 67 configurations. For the sake of simplicity, these configurations are only numbered from 1 to 67. The first 38 configurations are the ones with excitation along the Z axis, configurations 39–62 are for excitation along the X axis, and the configurations 63 upward are for excitation along the Y axis. The lines joining the values for the different configurations do not have any meaning by themselves and are included only to make the C^2 values easier to locate on the graph. The key observation from Fig. 8 is that the computed C^2 is basically independent of Q or damping for a large majority of cases. This finding is in agreement with the force limits derived from the more analytical simple TDFS method as shown in Fig. 2 of Ref. 2. According to the simple TDFS model, as long as the ratio of the effective mass of the test item over the effective mass of the mounting structure is above about 0.02 for the selected two Q values, the parameter equivalent to the C^2 of the semiempirical method is basically independent of Q. In the present study, no effective mass ratio was below 0.3. The relevant effective masses are the ones in the third octave frequency band encompassing the fundamental mode of the test item. For either the test item or the mounting structure, the effective mass for cases having more than one mode in the relevant third octave band was taken as the largest value of the effective masses in the band. Note that other approaches for the band effective mass have been proposed, such as taking the average[1] or the sum[20] of the masses in the band.

Table 1 Summary of occurrences of C^2 values

	Occurrences, %		
C^2 range	All cases	Lateral cases	Vertical cases
$C^2 < 2$	42	16	62
$C^2 < 5$	79	66	89
$C^2 < 10$	92	81	100
$C^2 < 20$	99	97	
$C^2 < 25$	100	100	

A summary of distribution of the derived exact C^2 values is presented in Table 1. The first column presents the five cumulative ranges in which the C^2 values are divided. The other columns present how the values are distributed for three different sets of cases. The second column presents the distribution in percentage of occurrence for all 134 cases considered. The third column considers only the results for the 58 cases for which the excitation is in the lateral directions (either X and Y axes), whereas the fourth column refers only to the 76 cases for which the excitation is in the Z direction. The numbers refer to the percentage of occurrences within the related C^2 range for the specified set, for example, 16% of all cases with excitation in the lateral directions has a C^2 value smaller than 2.

A first observation that may be made from the results of all cases is that all C^2 values are less than 25. This is a very interesting finding considering that the effective mass ratios span a range of several orders of magnitude. The very high effective mass ratios occur for the configurations for which there is negligible effective mass for the mounting structure in the third octave frequency band of the fundamental mode of the test item. A surprising result is that more than 40% of all cases, and especially more than 60% of the cases with excitation in the vertical direction, have a C^2 value lower than 2. For this lowest range of C^2, the effective mass ratio covers also

several orders of magnitude, starting with a ratio as low as 0.3 for excitation in the vertical direction.

For the 58 cases with excitation in the lateral directions, it is found that all C^2 values are less than 17, except for two cases of a single configuration giving values of 23 and 25 for the two different values of Q. Detailed analysis of the results reported in Ref. 13 shows that for the cases having the same number and position of interface attachment points, C^2 is inversely proportional to the effective mass ratio. This is to be expected because the vibration absorber effect should be more significant with the increased relative importance of the effective mass of the test item at its fundamental frequency relative to the relevant effective mass of the mounting structure. The simple TDFS model predicts this inverse proportionality relationship. However, it is found that the relationship between C^2 and the effective mass ratio is also dependent on the number and position of the attachment points. It is also observed that, for a specific number of attachment points, the value of C^2 varies with respect to the position of these attachment points. However, because changing the position of the same number of attachment points affects the effective mass ratio, it is difficult to discuss further the possible causes of this change other than saying that the resulting variation in structural stiffness is likely to influence the C^2 value. When the influence between C^2 and the effective mass ratio is considered, there are not enough data to come up with any definite conclusion concerning the relationship of the C^2 value with respect to the number of attachment points.

For the 76 cases with excitation in the vertical direction, it is observed from Table 1 that almost 90% of the values of C^2 are below 5 and all of them are below 10. Detail analysis of the results does not allow any specific conclusion on the relationship between C^2 and the effective mass ratio. The reason is that, for some attachment point configurations, C^2 decreases with an increase of the mass ratio as expected, whereas C^2 is surprisingly proportional to the mass ratio for some other configurations. The reason for the latter relationship, which is completely different than the behavior predicted from the simple TDFS model, is likely to be found in the difference between the attachment point configurations. For the cases having lateral excitation, all interface attachment points are within the same plane with respect to the base excitation and the center of gravity of the test item and the mounting structure. Consequently, these configurations are quite similar with the one of the TDFS model for which the two oscillators are sequentially attached at a single attachment point. On the other hand, the attachment points for the cases with excitation in the vertical direction are located all around the axes of the c.g. of the two structures, instead of being in the same plane. Because the detailed results of Ref. 13 show configurations with the same number of attachment points at different locations having similar effective mass ratios (thus, eliminating this variable in the equation), it was possible to observe the relationship between the position of the attachment points and the resulting C^2 value. In fact, it is found that the position of the attachment points has a significant influence on the value of C^2: For almost all cases, its value is lower when the attachment points are located where the mounting structure exhibits more flexibility than where it is more rigid. As for the cases with excitation in the lateral direction, no definite conclusion concerning the relationship between the C^2 value and the number of attachment points can be made.

From Table 1, one may observe that the values of C^2 are globally significantly lower for the cases with excitation in the vertical direction than for those with excitation along the horizontal lateral directions. When one compares the values of C^2 for each configuration common to both vertical and lateral directions, it is found that for the large majority of them C^2 is lower for the excitation along the vertical direction. A possible explanation could be that, for all configurations (with one exception), the test item is more rigid in the vertical direction than in the lateral direction as confirmed by the higher value of the fundamental frequency. However, this explanation can not be readily demonstrated with the considered cases due to the various causes affecting the C^2 values.

In concluding the discussion on the C^2 value, note the following three points. First, cases with effective mass ratios lower than 0.3, that is, the minimum value considered in this study, would likely result in C^2 values that are larger than the ones presented in Table 1. The value of 100 cited in the Introduction for the very light assembly of the Hubble Wide Field Planetary Camera represents an extreme such case. Second, as mentioned before, the numbers presented here are for the exact values of C^2 assuming enveloping of system interface acceleration and force was performed exactly. For conservatism purposes, one might consider adding some margin to such numbers, in a similar manner as margin is added in defining acceleration input profile. Third, the results of Table 1 gives an indication of the range of C^2 values that might be expected. In real life situation, the final selection of C^2 is based on the application of various criteria or guidelines such as comparison with the quasi-static limit load factor, observation of the amount of the peak force PSD being eliminated from the application of the force limits, and comparison with force limits derived from the TDFS methods.

For all cases considered, the depth of notching of the input acceleration at the fundamental or most significant mode of the test item were also computed. For a Q of 20, the range of almost all notching values was from 11 to 28 dB. The only exception was a notching of 6 dB for the configuration discussed earlier that had a high C^2 value above 20. For a Q of 50, the range of all notching was from 14 to 33 dB. These large numbers definitively give an indication of the amount of overtesting present in conventional vibration testing, when no input notching is incorporated in the control strategy.

VII. Experimental Validation of Analytical Procedures

The analytical sensitivity study was followed by an experimental phase aimed at validating the analytical procedures conducted in the study. This validation was done by comparing, for a few selected cases of the sensitivity study, the C^2 values derived experimentally with the corresponding values obtained analytically. All details of the experimental phase of the work are presented in Ref. 13.

Based on some guidelines developed to optimize the experimental work, 16 different analytical cases were tested. These cases are grouped into 6 configurations with lateral horizontal excitation in the X direction and 10 configurations with vertical excitation. To perform the comparison between the analytical and experimental results, the FE model of the test item for some of the selected configurations had to be slightly modified and the procedures for estimating the analytical C^2 value run again. These analytical modifications were either changes in position of the lumped masses or in the type of stiffening members. These changes were required 1) due to some interference between lumped masses mounted to the middle plate and 2) in response to one of the guidelines requiring to maximize the number of cases using the same stiffening members.

There were several steps involved in the test program. These steps were essentially the same for all configurations. They included the following steps:

1) Validation of the test fixtures was performed with low-level vibration tests.

2) A driven-base modal survey with low-level burst random excitation of the mounting structures was used to correlate the FE model.

3) Driven-base low-level random testing (flat spectrum with 1-g rms) of the test items was performed to obtain the apparent mass and the fundamental frequency and to correlate the FE model.

4) System-level random vibration testing was performed at 3.5-g rms, using a scaled-down level of the GEVS profile described earlier. Testing was performed at a lower level than what the structures were designed for to avoid undue damage caused by fatigue because numerous tests were done. The interface accelerations were monitored at each attachment point. The interface force was obtained by summing up the force at each of the attachment points measured by triaxial force sensors.

5) The test-based C^2 value was calculated based on system-level interface acceleration and force PSDs, using the same procedures as applied for the analytical sensitivity study.

The results of the experimental work are presented in this section for the cases involving excitation along the vertical direction. The cases involving excitation in the lateral direction did not provide

Table 2 Comparison of test-based and analytical parameters, including C^2 values

Case	Case name	% Difference in fundamental frequency		C^2 values	
		MS	Test Item	Experimental	FE model
1	4pt_4r_two_mwl	9.0	16.4	3.1	3.8
2	4pt_4r_two_2mwl	*[a]	16.4	3.0	3.2–3.8
3	4pt_4r_two_mwo	3.0	16.4	3.0	3.4–3.6
4	4pt_4r_twl1_2mwl	*	21.1	11	14
5	4pt_4r_twl2_2mwl	*	21.1	2.7	7.0
6	8pt_4r4o_two_mwl	9.0	8.8	1.1	0.8
7	8pt_4r4o_two_2mwl	*	8.8	0.92	0.86
8	8pt_4r4o_two_mwo	3.0	8.8	1.6	0.9–0.8
9	8pt_4r4o_twl_mwl	9.0	8.5	——	——
10	4pt_4o_two_2mwl	*	11.1	7.2	6.5–6.4

[a]*, No experimental value available; see the text.

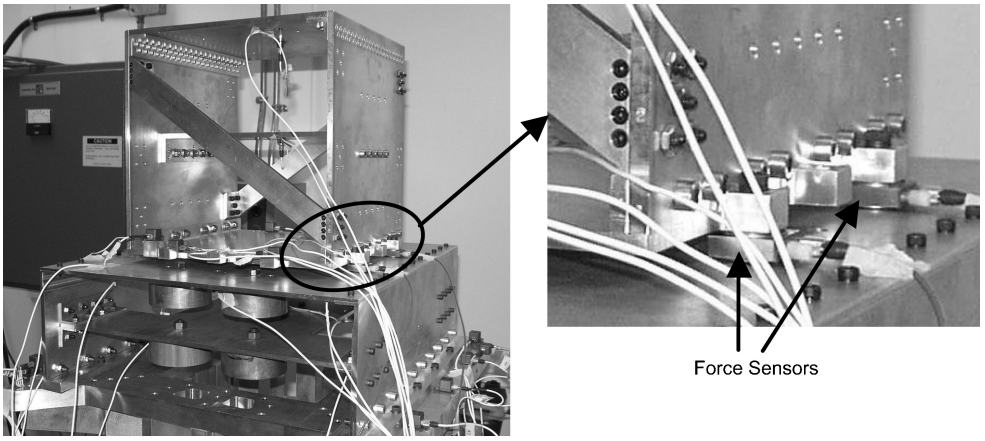

Fig. 9 Setup for system-level vibration testing.

conclusive results and, therefore, are not shown for the sake of brevity. This inability of the latter results to validate the procedures used in analytical study was traced back to a lack of fidelity of the FE model of the mounting structures compared to the physical model. The FE model infidelity was confirmed by a discrepancy of more than 30% between the analytical and experimental fundamental frequencies of the mounting structures in the lateral direction. Model updating was not performed due to budget and especially time constraints and, more important, because the results with excitation in the vertical direction are considered sufficient to achieve the objective of the experimental part of the work, that is, to validate the analytical procedures.

Figure 9 shows the setup of system-level vibration testing for one of the configurations. The force sensors located at the two interface attachment points of the right sidewalls are clearly visible. The accelerometers measuring the interface accelerations are not visible because they were installed underneath the top plate of the mounting structure. Several of the accelerometers fixed to the two structures and the fixture are shown in Fig. 9. They include the ones on the top and middle plates of the test item. As may be observed, in this configuration, the test item has no lumped mass, whereas some are attached to the mounting structure. This configuration is named 4pt_4r_two_mwl.

The comparison between the test-based and analytical parameters, including the C^2 values, is presented in Table 2. The name of the various configurations is shown in the second column. The first parameter in the name refers to the number of interface attachment points. The second parameter of the name describes the position of these attachment points. For example, 4r implies that all attachment points were located on the side of the sidewalls of the test item (two on each side), whereas 4r4o indicates that four attachment points were on the side of the sidewalls and four more points were on the sides orthogonal to the sidewalls. The third parameter indicates whether there is lump mass attached to the test item: Here two means without lump mass, whereas twl indicates a test item with lumped mass. For the fourth and fifth cases, a number is added at the end of the third parameter because there is a small difference in the position of the lumped mass: In case 4, most of the mass is added on the top plate; in case 5, the mass is distributed more evenly between the top and middle plates. Similarly, the fourth parameter of the name indicates if there is lump mass attached to the mounting structure: Here mwo means without lump mass, whereas mwl indicates a mounting structure with lumped mass attached to the top and middle plates. When additional lump mass is attached to the side plates, this parameter is called 2mwl.

The third and fourth columns of Table 2 present the percentage difference in the fundamental frequencies for the mounting structures (MS) and test items, respectively. These values are obtained by taking the experimental frequency as the reference. For the MS, an * is shown for the configuration for which lumped mass was added to the side plates because no experimental value is available. The modified MS configuration was decided after the testing of the structure. It is only after completion of the test program that it was realized that the test data were missing to correlate the FE model in this configuration. For programmatic reasons, it was not feasible to go back to testing to obtain the missing information. In any case, the percentage difference in the fundamental frequency for the 2mwl configuration is expected to be similar to the mwl configuration, that is, about 9%. Note that there exists a very good agreement between the analytical and experimental fundamental frequencies of the MS, especially considering that no model updating was performed. For the fundamental frequencies of the test items, although the agreements are not as good as for the MS, they are considered acceptable considering the purpose of the experimental work. Note that a better agreement is obtained for the configurations with eight attachment points than for those with only four attachment points.

The C^2 values from testing are shown in the fifth column. The values in the last column indicate the range of analytical values. The first and second values were obtained when the test item and MS are assumed to have a Q of 20 and 50, respectively. When only one value is shown, it was obtained for a Q of 50. Observe that there is very good agreement for most cases. For case 4, the larger discrepancy is still quite acceptable. Also for this case, it is observed that the fairly large value for C^2 derived from analysis is indeed confirmed by its test-based counterpart. Case 5 shows by far the largest discrepancy. This anomaly in the comparison is explained by a discrepancy between the FE model and the physical model with respect to how the middle plate of the test item is attached to the sidewalls. In this particular case, the lumped mass is distributed evenly between the top plate and middle plates. It has been realized that the fundamental mode of the test item by itself is driven by the middle plate for both the analytical and experimental work. However, at the system level, the mode corresponding to the peak adjacent to the antiresonance (corresponding to the fundamental frequency of the test item by itself) is driven by the top plate in the analysis and by the middle plate in the experimental work. For case 9, no value for C^2 could be obtained from either the analysis or the test. The reason is that the interface accelerations and the forces at the system level could not be extracted from the PSD data because the mode corresponding to the peak adjacent to the antiresonance got mixed with the system-level modes.

Based on the results of Table 2 and the discussion in the preceding paragraphs, it is concluded that the experimental work does validate the procedures used for the analytical sensitivity study and, consequently, the C^2 values derived in the study.

VIII. Conclusions

This paper presents the main results and findings of a research and development project investigating the semiempirical method of FLV testing, especially the range of values taken by the key constant C (or C^2) and the parameters on which it depends. The paper includes the details and the results of an in-depth analytical sensitivity study with 134 different cases and the results of the experimental validation of the analytical procedures using some of the cases of the analytical study. The cases of the analytical study consist of 67 different configurations with two different Q values (20 and 50).

The analytical sensitivity study shows that, for the 58 cases with excitation in the lateral directions, the majority of C^2 values are less than 5 and almost all of them are less than 17. For the 76 cases with excitation in the vertical direction, the C^2 values are even smaller with the majority of them being less than 2 and all of them being less than 10. In real-life situations, the selected C^2 values are likely to be higher because one might add some margin for conservative purposes, in a similar manner as margin is added in defining acceleration input profile.

From the analytical sensitivity study, it is observed that C^2 is basically independent of the damping value for most configurations. Also, it is found that the C^2 value depends mainly on the following parameters:

First is the effective mass ratio between the test item and the mounting structure, in the frequency band of the fundamental frequency of the test item. The effective mass ratios considered in the study span a range of several orders of magnitude, starting with a minimum value of 0.3. For the cases with excitation in the lateral directions having the same number and position of interface attachment points, C^2 is inversely proportional to the effective mass ratio, as predicted by the analytical simple TDFS method. However, it is found that this inverse proportionality relationship is also dependent on the number and position of the attachment points. For the cases with excitation in the vertical direction, the results of the study do not allow any specific conclusion on the relationship between C^2 and the effective mass ratio.

Second is the position and number of the interface attachment points between the test item and the mounting structure. The study shows that the position of the attachment points has a significant influence on the value of C^2 for the cases with excitation in the vertical direction. For almost all of these cases, the C^2 value is lower when the attachment points are located where the mounting structure exhibits more flexibility. Concerning the effect of the number of attachment points on the C^2 value, there is not enough similar cases to come up with a clear conclusion, although it is observed that this parameter has definitely an influence.

Last is the direction of excitation. It is observed from the study that the values of C^2 are globally significantly lower for the cases with excitation in the vertical direction than for those with excitation along the horizontal lateral directions. When one compares the values of C^2 for each configuration common to both vertical and lateral directions, it is found that for the large majority of them C^2 is lower for the excitation along the vertical direction.

The level of notching of the input acceleration to the test item caused by force limiting confirms the significant amount of overtesting present in conventional vibration testing without notching. For almost all considered cases and for a Q of 20, the notching of the input acceleration PSD is found to be between 11 and 28 dB. For a Q of 50, the notching level is even larger, as expected.

Acknowledgments

Partial support by Natural Science and Engineering Research Council of Canada is gratefully acknowledged. The authors thank Daniel Lévesque of the Canadian Space Agency (CSA) Space Technologies Sector for discussions concerning the design and analysis of the test structures. We acknowledge André Côté, formerly with EMS Technologies, for suggesting the approach used in the analytical study for deriving the total interface force. We also thank Raj Singhal of the CSA David Florida Laboratory for the loan of some of the force sensors used in the experimental part of the work.

References

[1]Scharton, T. D., "Force Limited Vibration Testing Monograph," Jet Propulsion Lab., NASA RP 1403, Pasadena, CA, May 1997.

[2]"Force Limited Vibration Testing," Jet Propulsion Lab., NASA Technical Handbook, NASA-HDBK-7004B, Pasadena, CA, Jan. 2003.

[3]Scharton, T. D., "In-Flight Measurements of Dynamic Force and Comparison With Methods Used to Derive Force Limits for Ground Vibration Tests," *Proceedings of the European Conference on Spacecraft Structures, Materials and Mechanical Testing (A00-17601 03-18)*, ESA Publ. Div., Noordwijk, The Netherlands, 1999, pp. 583–588.

[4]Scharton, T. D., "Force Limits Measured on a Space Shuttle Flight," *Journal of the IEST*, Vol. 45, No. 1, 2002, pp. 144–148.

[5]Worth, D. B., and Kaufman, D. S., "Validation of Force-Limited Vibration Testing," *Journal of the IEST*, Vol. 41, No. 3, 1998, pp. 17–23.

[6]Kaufman, D. S., and Worth, D. B., "Follow on Validation of Force-Limited Vibration Testing," *Proceedings of the 19th Aerospace Testing Seminar*, Inst. of Environmental Sciences and Technology, Mount Prospect, IL, 2000, pp. 338–351.

[7]Chang, K. Y., "Force Limit Specifications vs. Design Limit Loads in Vibration Testing," *Proceedings of the European Conference on Spacecraft Structures, Materials and Mechanical Testing*, ESA Publ. Div., Noordwijk, The Netherlands, 2001, pp. 295–300.

[8]Scharton, T. D., and Lee, D., "Random Vibration Test of Mars Exploration Rover (MER) Flight Spacecraft," 2003 S/C and L/V Dynamic Environments Workshop, www.aero.org/conferences/sclv/2003-proceedings.html [accessed 15 May 2006].

[9]Soucy, Y., Singhal, R., Lévesque, D., Poirier, R., Scharton, T. D., "Force Limited Vibration Testing Applied to the Fourier Transform Spectrometer Instrument of SCISAT-1," *Canadian Aeronautics and Space Journal*, Vol. 50, No. 3, 2004, pp. 189–197.

[10]Sweitzer, K. A., "A Mechanical Impedance Correction Technique for Vibration Tests," *Proceedings of the 33rd ATM*, Inst. of Environmental Sciences, San Jose, CA, 1987, pp. 73–76.

[11]Soucy, Y., Dharanipathi, V. R., and Sedaghati, R., "Investigation of Limit Criteria for Force Limited Vibration," 2005 Spacecraft and L/V Dynamic Environments Workshop, http://www.aero.org/conferences/sclv/2005proceedings.html [accessed 15 May 2006].

[12]Soucy, Y., and Chesser, H., "Force Limited Vibration Testing Applied to the MOST Spacecraft," *Canadian Aeronautics and Space Journal*, Vol. 51, No. 2, 2005, pp. 47–60.

[13]Dharanipathi, V. R., "Investigation of the Semi-Empirical Method for Force Limited Vibration Testing," M.S. Thesis, Dept. of Mechanical and Industrial Engineering, Concordia Univ., Montreal, Sept. 2003.

[14]*MSC.Patran 2001 User's Guide for UNIX*, MSC Software Corp., Santa Ana, CA, 2001.

[15]Herting, D. N., *MSC/NASTRAN Version 70 Advanced Dynamic Analysis User's Guide*, MacNeal–Schwendler Corp., Santa Ana, CA, 1997.

[16]"Femap & Femap with NX Nastran Features," UGS, URL: http://www.ugs.com/products/velocity/femap/features.shtml [accessed 15 May 2006].

[17]"General Environmental Verification Specification for STS and ELV, Payloads, Subsystems, and Components," GEVS-SE, Rev. A, NASA, Greenbelt, MD, June 1996, pp. 2.4–19.

[18]Soucy, Y., Dharanipathi, V. R., and Sedaghati, R., "On the Semi-Empirical Method for Force Limited Vibration," 2004 Spacecraft and L/V Dynamic Environments Workshop, www.aero.org/conferences/sclv/2004-proceedings.html [cited 15 May 2006].

[19]Soucy, Y., Dharanipathi, V. R., and Sedaghati, R., "Comparison of Methods for Force Limited Vibration Testing," IMAC 23rd Conf. and Exposition on Structural Dynamics, Society for Experimental Mechanics, Paper 295, Jan.–Feb. 2005.

[20]Côté, A., Sedaghati, R., and Soucy, Y., "Force-Limited Vibration Complex Two-Degree-of-Freedom System Method," *AIAA Journal*, Vol. 42, No. 6, 2004, pp. 1208–1218.

L. Peterson
Associate Editor